

# A Bisected Miniaturized ZOR Antenna With Increased Bandwidth and Radiation Efficiency

Shu-Yen Yang and Malcolm Ng Mou Kehn, *Member, IEEE*

**Abstract**—A compact planar, via-free, and bisected zeroth-order resonator (ZOR) antenna based on bisected interdigital capacitor-loaded transmission line (B-CL-TL), with improved bandwidth and higher radiation efficiency is proposed. Strong miniaturization and increase of bandwidth and efficiency are obtained by dissecting the initial design by half without incurring compromise. The antenna consists of two cascaded coplanar interdigital capacitors as series capacitors shorted to the ground plane at one end. A meander-line inductor is implemented for matching. A fabricated prototype has dimensions of  $0.11\lambda_0 \times 0.18\lambda_0 \times 0.01\lambda_0$  in total size, yielding an omnidirectional far-field pattern, and provides a 135-MHz bandwidth (6.1%) with a measured radiation efficiency of 76.8% at 2.21 GHz.

**Index Terms**—Antenna miniaturization, bandwidth enhancement, interdigital capacitor (IDC), radiation efficiency, zeroth-order resonator (ZOR) antenna.

## I. INTRODUCTION

THE QUEST for applications of metamaterials at microwave frequencies is an extensive research area due to their unique properties such as antiparallel propagation properties [1], [2] and zeroth-order resonance (ZOR) [2]. An interesting situation relates to the ZOR, whereby the propagation constant vanishes at a nonzero frequency. This implies that the resonance condition becomes independent of the physical dimensions of the antenna, but depends only on the amount of reactance provided by its unit cells. Therefore, ZOR provides a support for convenient antenna miniaturization techniques as their unit cells can be kept electrically small by employing interdigital or lumped reactive circuit elements [3]. The composite right/left-handed transmission line (CRLH-TL) architecture has been proposed for realizing the ZOR antenna [4]. Since only either shunt or series resonances can be practical for CRLH TL for either open- or short-end condition, respectively, reduction of ohmic losses and structural complexity can be achieved by removing the resonance that is not used. Based on this concept, two distinct structures—inductor-loaded transmission line (IL-TL) and capacitor-loaded transmission line (CL-TL) in coplanar structure—were reported in [5]. We are herein interested only in the CL-TL for attaining higher efficiencies based

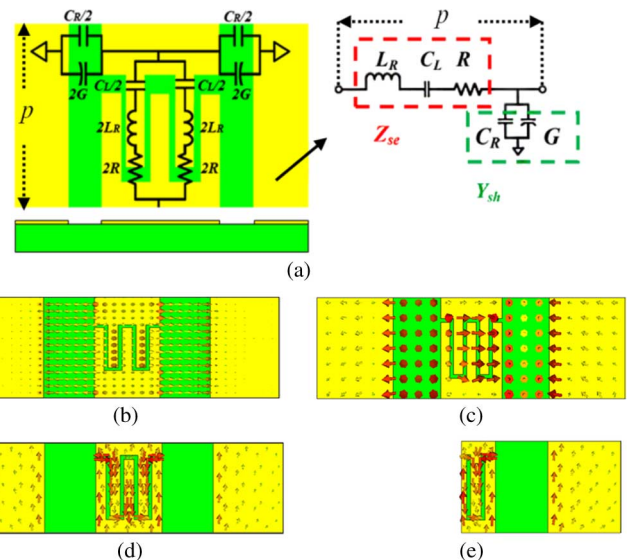


Fig. 1. (a) Geometry of the coplanar CL-TL with potential for zeroth-order resonance and equivalent circuit model of the unit cell. (b) E-field distribution symmetric about the vertical plane. (c) H-field distribution anti-symmetric about the vertical plane. (d) Surface current distribution of CL-TL. (e) Surface current distribution of bisected CL-TL (B-CL-TL).

on a simple structure, as schematized in Fig. 1(a). Although ZOR antennas offer the advantage of size reduction, they suffer from narrow bandwidths. To solve this problem, the merging of two bands based on spiral-inductor-loaded transmission-line metamaterial (TL-MTM) was proposed in [6]. However, this method increases the antenna dimensions. Symmetric bisection of the antenna has been a resort to reduce the size [7], [8]. However, as far as the authors are aware, there are no works that focus on the changes in the bandwidth and radiation efficiency associated with this miniaturization technique. In this letter, we reduce the dimensions and  $Q$  of the CL-TL ZOR antenna by cutting it into half. Generally,  $Q$  is the inverse of the bandwidth and radiation efficiency. Therefore, bisecting the antenna not only provides miniaturization, but also increases the bandwidth and radiation efficiency. Moreover, an omnidirectional radiation pattern in the vertical plane is achievable. In this letter, we provide an effective way not only to miniaturize ZOR antennas, but also to extend their bandwidths and enhance the radiation efficiencies.

## II. ANTENNA THEORY AND DESIGN

### A. Basic Theory of CL-TL ZOR Antenna

Referring to [3], a zeroth-order resonator can be obtained by loading a capacitor [ $C_L$  of Fig. 1(a)] in series with the inherent inductor ( $L_R$ ) of a typical resonant transmission line

Manuscript received October 13, 2012; revised December 11, 2012; accepted January 22, 2013. Date of publication January 29, 2013; date of current version March 12, 2013.

S.-Y. Yang is with the Department of Electrical Engineering, National Chiao Tung University, Hsinchu 30010, Taiwan.

M. Ng Mou Kehn is with the Department of Electrical and Computer Engineering, National Chiao Tung University, Hsinchu 30010, Taiwan (e-mail: malcolm.ng@iee.org).

Color versions of one or more of the figures in this letter are available online at <http://ieeexplore.ieee.org>.

Digital Object Identifier 10.1109/LAWP.2013.2243696

under a shorted-end condition. Similarly, loaded inductors and inherent capacitors also can produce zeroth-order resonance in open-ended condition. The equivalent circuit model of the unit cell is shown in Fig. 1(a). The overall series element,  $Z_{se}$  and shunt element,  $Y_{sh}$ , as also shown in Fig. 1(a) are given by

$$Z_{se} = R + j(\omega L_R - 1/\omega C_L) \quad (1)$$

$$Y_{sh} = G + j\omega C_R. \quad (2)$$

For a TL of length  $l$  [=  $Np$ , whereby  $N$  is the number of unit cells and  $p$  is the length of the unit cell as indicated in Fig. 1(a)] under lossless and shorted-end condition, its associated  $Z_{in}$  is given by

$$\begin{aligned} Z_{in}^{short} &= jZ_c \tan \beta l \stackrel{\beta \rightarrow 0}{\approx} jZ_c \beta l \\ &= j\sqrt{\frac{Z_{se}}{Y_{sh}}} \left( \frac{\sqrt{Z_{se}Y_{sh}}}{j} \right) l = Z_{se}l \end{aligned} \quad (3)$$

indicating the sole presence of  $Z_{se}$ , which upon referring to (1) reveals that the resonance frequency is given by

$$\omega_{se} = \frac{1}{\sqrt{L_R C_L}}. \quad (4)$$

Hence, the latter depends on the series part of the circuit. Because the equivalent circuit can be transformed to a series-type resonator circuit, the  $Q$  of this antenna can be calculated from the formula of the series resonator circuit given in

$$Q = \frac{2\omega_{se}W_e}{(P_{loss} + P_{rad})} = \frac{1}{\omega_{se}R C_L} = \left( \frac{1}{R} \right) \sqrt{\frac{L_R}{C_L}} \quad (5)$$

[assume that the stored electrical energy ( $W_e$ ) is equal to the stored magnetic energy ( $W_m$ )], where  $P_{loss}$  is the loss power, and  $P_{rad}$  is the total radiated power.

### B. B-CL-TL

According to the image theory [9], an electric source near a perfect magnetic (electric) conductor (PMC and PEC) is equivalent to two in-phase (out-of-phase) electric sources at the center without the PMC (PEC). For a magnetic source, on the other hand, the actual and image sources are out of phase from (in phase with) each other. As such, when the E- and H-fields are symmetric and anti-symmetric about a certain plane, this surface can be regarded as a PMC boundary. Fig. 1(b) and (c) shows the E- and H-field distributions of the coplanar CL-TL antenna that satisfy such a condition. Since PEC boundaries are on one hand equivalent to shorted ends, PMC boundaries on the other hand may be deemed as open-ended by duality. This suggests that we can get similar performance even though we bisect the antenna through its symmetry plane to obtain an open end, thus providing a simple and effective way to miniaturize the antenna dimensions. As shown by Fig. 1(d) and (e), the current distributions before and after the bisection are similar. After bisection, the input voltage, input current, and  $Z_{se}$  are unchanged, halved, and doubled, respectively. Theoretically, the parameters of the equivalent model upon halving are changed to [see Fig. 1(a)]

$$L'_R = 2L_R \quad C'_L = \frac{C_L}{2} \quad R' = 2R. \quad (6)$$

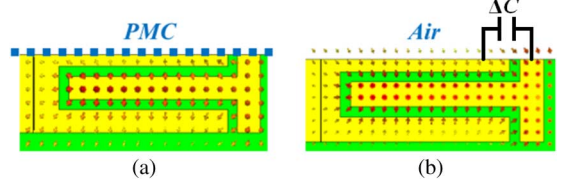


Fig. 2. Top view of the E-field distributions of the B-CL-TL: (a) theoretical scenario (PMC boundary) and (b) real (actual) scenario.

With these modifications applied to (4) and (5), i.e., unprimed replaced by the primed terms of (6), the  $Q$  and resonance frequency are seen to remain unchanged upon the bisection. However, Fig. 2(a) and (b), respectively portraying the top views of the hypothetical model of the interdigital capacitor (IDC) with a PMC boundary and its actual open-ended bisected scenario, show that more fields exist around the open-ended edge in the actual scenario than at the PMC boundary of the theoretical model.

Therefore, all  $L'_R$ ,  $C'_L$ , and  $R'$  of (6) must be corrected. According to Fig. 2(b), a corrective capacitance  $\Delta C$  should be considered in the real scenario. Fig. 1(e) shows that the surface current near the bisecting plane is not in the same direction. Therefore, the true resistance, say  $R''$ , after bisection should be amended to be greater than twice of  $R$ , in refinement of  $R'$  in (6). Likewise, according to the definition of inductance, which is flux linkage divided by the current, the true  $L'_R$ , say  $L''_R$ , is greater than  $2L_R$ . Hence, these actual (double-primed) parameters are stated as

$$R'' = aR' = 2aR \quad (7)$$

$$L''_R = bL'_R = 2bL_R \quad (8)$$

$$C''_L = cC'_L = \frac{cC_L}{2} \quad (9)$$

where  $a$ ,  $b$ , and  $c$  are the increment factors (greater than unity) of  $R'$ ,  $L'_R$ , and  $C'_L$ , respectively. Subsequently, the actual resonant frequency and actual  $Q$  denoted by  $\omega''_{se}$  and  $Q''$ , respectively, are written as

$$\omega''_{se} = \frac{1}{\sqrt{L''_R C''_L}} = \frac{\omega_{se}}{\sqrt{bc} < \omega_{se}} \quad (10)$$

$$Q'' = \left( \frac{1}{R''} \right) \sqrt{\frac{L''_R}{C''_L}} = \left[ \left( \frac{1}{a} \right) \sqrt{\frac{b}{c}} \right] \cdot Q \quad (11)$$

Hence, the actual  $Q''$  will indeed be less than the *unbisected*  $Q$ . Generally,  $Q$  is inversely proportional to the bandwidth and radiation efficiency. Therefore, we can obtain extended bandwidth and higher efficiency performance by halving the antenna. Note that (5) does not consider the matching network at the input terminals, but they still provide an intuitive concept that bandwidth and radiation efficiency can be increased effectively.

### C. Design of the Proposed Antenna

The unit cell of the proposed half-cut ZOR antenna, shown as an inset drawing in Fig. 3, is printed on an FR4 dielectric board with a thickness of 1.6 mm. The following equation:

$$\beta p = \cos^{-1} \left( \frac{1 - S_{11}S_{22} + S_{12}S_{21}}{2S_{21}} \right) \quad (12)$$

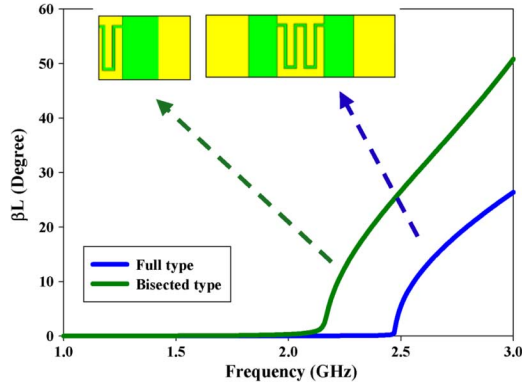


Fig. 3. Unit cells and dispersion curves generated by (12) derived from ABCD matrix theory, for full type and half type.

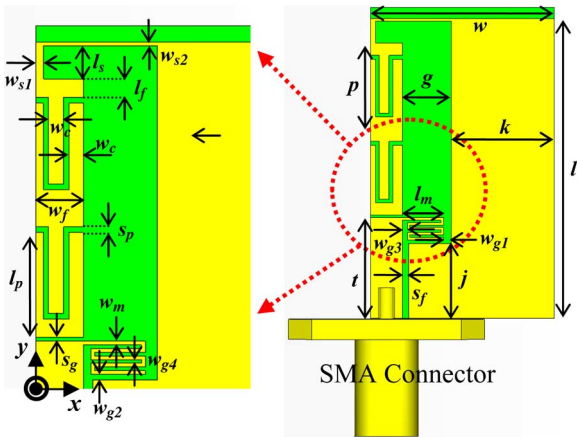


Fig. 4. Geometry of proposed B-CL-TL antenna.

which can be derived from ABCD matrix theory [9], provides a simple way to calculate the dispersion diagram, where  $p$  is the length of the unit cell as indicated in Fig. 1(a).

The dispersion diagram of the bisected type also in Fig. 3 shows the shift in the ZOR frequency from 2.45 GHz for its full uncut counterpart to 2.15 GHz. A schematic of the proposed B-CL-TL antenna is shown in Fig. 4, consisting of two cascaded coplanar IDC-loaded unit cells. All related structures were simulated in CST Microwave Studio. The feedline was connected to the coaxial cable through a standard 50- $\Omega$  SMA connector. The SMA connector was included in all simulations to characterize their effects on the antenna performance. To improve the matching, a meander line serving as a series inductor is added to the end of the feedline. Design parameters of the proposed antenna are given in Table I. The larger the distance [ $g$ , which is shown in Fig. 4(a)] between the IDC and the coplanar ground of the coplanar waveguide (CPW), the larger will be the achievable efficiency as more fields radiate out into the air instead of toward the ground. From ABCD matrix theory [4], we can extract the equivalent circuit parameters under lossy conditions as shown in Table II. According to Table II, we can calculate  $Q$  and prove the inference in Section II-B: that the *bisected antenna can achieve lower  $Q$* .

### III. SIMULATION AND EXPERIMENTAL RESULTS

Prototypes of both the full-type and bisected antennas were fabricated, as photographed in Table III. The simulated ZOR

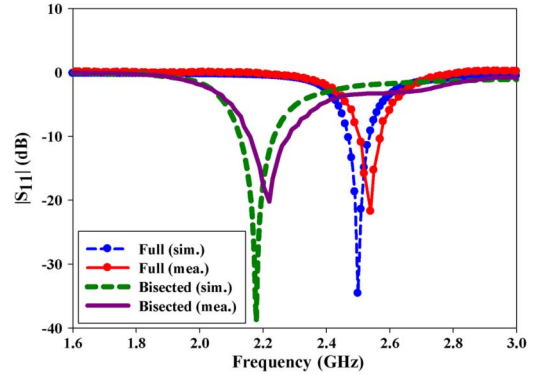


Fig. 5. Simulated and measured  $|S_{11}|$  of CL-TL and B-CL-TL ZOR antenna.

TABLE I  
DESIGN PARAMETERS (UNITS: MILLIMETERS)

$w$	15	$k$	8.4	$w_{s1}$	0.4	$l_f$	1	$w_{g2}$	0.3
$l$	24.4	$j$	6.1	$w_{s2}$	0.2	$l_p$	5.7	$w_{g3}$	0.4
$p$	7	$s_f$	0.5	$s_p$	0.3	$s_g$	0.2	$w_{g4}$	0.2
$g$	4	$l_m$	3.35	$w_c$	0.8	$w_m$	0.2		
$t$	8.2	$l_s$	1.8	$w_f$	2.6	$w_{g1}$	0.65		

TABLE II  
EQUIVALENT CIRCUIT PARAMETERS

	Full	Half
$f_0$ (GHz)	2.45	2.15
$R$ (Ohm)	1.7	5
$L_R$ (nH)	3.17	6.85
$C_I$ (pF)	1.33	0.8

TABLE III  
COMPARISON OF MEASURED PERFORMANCES BETWEEN FULL AND BIASECTED VERSIONS

	CL-TL ZOR	B-CL-TL ZOR
$f_0$ (GHz)	2.45	2.15
B.W. (%)	3	6.1
$\eta$ (%)	52	76.8
Size ( $\lambda_0 \times \lambda_0$ )	0.25 $\times$ 0.2	0.11 $\times$ 0.18

frequency is 2.15 GHz, and the bandwidth, efficiency, and gain are 110 MHz (5.1%), 84%, and 2.24 dBi, respectively. The measured ZOR frequency is 2.21 GHz, and the measured bandwidth is 135 MHz (6.1%). The simulated and measured ZOR frequencies and their associated bandwidths for both the full and bisected versions are given in Fig. 5. The E-plane is the  $xy$ -plane, which has an omnidirectional pattern, whereas the H-plane is the  $xz$ -plane (see Fig. 4 for the coordinate system) with an isotropic pattern. Both of these are shown in Fig. 6. The measured peak gain is 1.4 dBi, and the efficiency is 76.8% from measurements



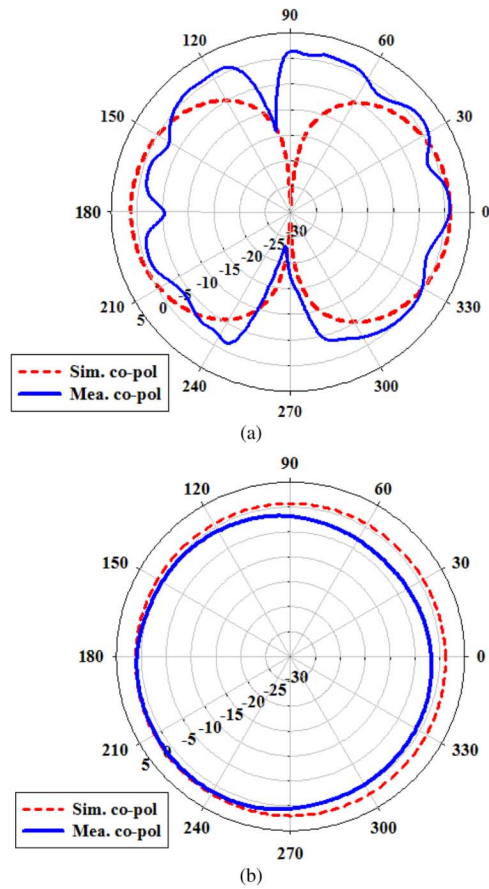


Fig. 6. Simulated and measured radiation patterns of the proposed bisected antenna at its zeroth-order resonator frequency. (a) E-plane:  $xy$ -plane. (b) H-plane:  $xz$ -plane.

TABLE IV  
COMPARISON RESULTS OF PROPOSED AND REFERENCE ANTENNAS

	Proposed	[10]	[11]	[12]
$f_0$ (GHz)	<b>2.21</b>	2.97	2.03	2.42
$\epsilon_r$	<b>4.4</b>	4.4	2.2	2.2
$\tan\delta$	<b>0.02</b>	0.02	0.0009	0.0009
Area ( $\lambda_0 \times \lambda_0$ )	<b>0.11x0.18</b>	0.22x0.22	0.15x0.17	0.08x0.22
$\eta$ (%)	<b>76.8</b>	75	66	53
B.W. (%)	<b>6.1</b>	1.9	6.8	1
Gain (dBi)	<b>1.4</b>	3.07	1.35	-0.53

in an anechoic chamber. Table III compares the measured performances of the CL-TL ZOR antenna and B-CL-TL ZOR antenna made up of the same materials. Compared to the CL-TL ZOR antenna, the size reduction, increase of bandwidth, and rise in radiation efficiency is 60%, 3.1%, and 24%, respectively.

Table IV summarizes and compares the performance of the proposed ZOR antenna with other designs found in literature. The manufactured antennas of the various referenced works in Table IV all consist of two unit cells. The format of the stated dimensions is width  $\times$  length. Compared to other types of ZOR antennas using lower-loss materials, e.g. [11] and [12], our proposed antenna has better performance in general despite being implemented on an FR4 substrate with higher loss except for

narrower bandwidth than [10]. For works employing the same dielectric material (FR4) such as [10], our design compares favorably to them both in terms of all aspects except just the gain, which is larger than our design, although [10] has taken the unfair advantage of using larger dimensions.

Therefore, our bisected ZOR antenna has demonstrated strong potential for designing compact antennas with extended bandwidth and higher radiation efficiency.

#### IV. CONCLUSION

In this letter, a very simple but effective way to miniaturize and enhance the bandwidth and efficiency of symmetric ZOR antennas is presented. By bisecting the symmetric ZOR antenna with a shorted end, the  $Q$  decreases strongly. Therefore, it overcomes disadvantages of compact antennas such as narrow bandwidth and low efficiency. The proposed B-CL-TL ZOR antenna, which is implemented on FR4, has a via-free uniplanar structure and shows a measured gain of 1.4 dBi, efficiency of 76.8%, and fractional bandwidth of 6.1%. The dimension of the total structure is  $0.11\lambda_0 \times 0.18\lambda_0 \times 0.01\lambda_0$ . The radiation pattern is omnidirectional in the vertical plane. Our proposed bisected ZOR antenna is thus a fine compact antenna design example as it attains the three key objectives (compact dimensions, increased bandwidth, and enhanced efficiency) simultaneously with a single elegant move (bisection).

#### REFERENCES

- [1] G. V. Eleftheriades, A. K. Iyer, and P. C. Kremer, "Planar negative refractive index media using periodically LC loaded transmission lines," *IEEE Trans. Microw. Theory Tech.*, vol. 50, no. 12, pp. 2702–2712, Dec. 2002.
- [2] A. Sanada, C. Caloz, and T. Itoh, "Characteristics of the composite right/left-handed transmission line," *IEEE Microw. Wireless Compon. Lett.*, vol. 14, no. 2, pp. 68–70, Feb. 2004.
- [3] J. Volakis, C. C. Chen, and K. Fujimoto, *Small Antennas: Miniaturization Techniques & Applications*. New York, NY, USA: McGraw-Hill, 2010.
- [4] C. Caloz and T. Itoh, *Electromagnetic Metamaterials: Transmission Line Theory and Microwave Applications*. New York, NY, USA: Wiley, 2005.
- [5] C. P. Lai, S. C. Chiu, H. J. Li, and S. Y. Chen, "Zeroth-order resonator antennas using inductor-loaded and capacitor-loaded CPWs," *IEEE Trans. Antenna Propag.*, vol. 59, no. 9, pp. 3448–3453, Sep. 2011.
- [6] J. Zhu and G. V. Eleftheriades, "A compact transmission line metamaterial antenna with extended bandwidth," *IEEE Antenna Wireless Propag. Lett.*, vol. 8, pp. 295–298, 2009.
- [7] R. Chair, C. L. Mak, K. F. Lee, K. M. Luk, and A. A. Kishk, "Miniature wide-band half U-slot and half E-shaped patch antennas," *IEEE Trans. Antennas Propag.*, vol. 53, no. 8, pp. 2645–2651, Aug. 2005.
- [8] L. Guo, S. Wang, X. Chen, and C. Parini, "Miniaturised antennas for UWB communications," in *Proc. Eur. Microw. Conf.*, Mar. 2009, pp. 3774–3778.
- [9] D. M. Pozar, *Microwave Engineering*, 2nd ed. New York, NY, USA: Wiley, 1998.
- [10] H. M. Lee and T. J. Cho, "Co-planar waveguide-fed zeroth-order resonant antenna with improved gain and efficiency," in *Proc. iWAT*, Hong Kong, Mar. 2011, pp. 388–391.
- [11] T. Jang, J. Choi, and S. Lim, "Compact coplanar waveguide (CPW)-fed zeroth-order resonant antennas with extended bandwidth and high efficiency on vialess single layer," *IEEE Trans. Antennas Propag.*, vol. 59, no. 2, pp. 363–372, Feb. 2011.
- [12] C. C. Liu, P. L. Chi, and Y. D. Lin, "Compact zeroth-order resonant antenna based on dual-arm spiral configuration," *IEEE Antennas Wireless Propag. Lett.*, vol. 11, pp. 318–321, 2012.